國立交通大學

電子工程學系電子研究所

碩 士 論 文

退火效應對螺旋式電感感值變化之研究

The Investigation of Annealing Effect on the Inductance Variance of On-Chip Spiral Inductor

研 究 生：賴 文 駿

指導教授：鄭 裕 庭　教授

中 華 民 國 九 十 六 年 七 月

退火效應對螺旋式電感感值變化之研究

The Investigation of Annealing Effect on the Inductance Variance of On-Chip Spiral Inductor

研 究 生：賴文駿　　Student：Wen-Chun Lai

指導教授：鄭裕庭　　Advisor：Yu-Ting Cheng

國 立 交 通 大 學

電子工程學系電子研究所

碩 士 論 文

A Thesis

Submitted to **Department of Electronics Engineering & Institute of Electronics**

College of Electrical and Computer Engineering

National Chiao Tung University

in Partial Fulfillment of the Requirements

for the Degree of Master

In

Electronics Engineering

July 2007

Hsinchu, Taiwan, Republic of China

中華民國九十六年七月

退火效應對螺旋式電感感值變化之研究

學生：賴文駿　　指導教授：鄭裕庭教授

國立交通大學電子工程學系電子研究所碩士班

摘　要

在這篇論文裡，主要是研究退火的效應對螺旋式電感的影響，在 30 分鐘還有 600 度 C 的退火溫度操作下，發現銅大約有 7.4%的電阻值下降，但是對於同樣製作在同一片晶片上的電感而言，電感感值幾乎沒有發生變化。十組 3.5 圈的螺旋式電感中，退火前後的電感感值差異有- 2.25%到 0.41%的變化，同時共振頻率有- 8.22%到 1.68%的變化。對於這樣的改變，我們利用統計學上的方法來做檢定，檢定的結果認為此變化會來自於實驗的誤差，事實上退火效應對電感是不會造成影響。而這樣的結果也顯示導電率與螺旋式電感感值沒有相關性，此研究符合 Greenhouse 電感感值公式的預測，而非 Chen et al.的模型。

The Investigation of Annealing Effect on the Inductance Variance of On-Chip Spiral Inductor

Student：Wen-Chun Lai　　Advisors：Yu-Ting Cheng

Department of Electronics Engineering ＆ Institute of Electronics

College of Electrical and Computer Engineering

National Chiao Tung University

Abstract

In At this paper, thermal annealing effect on the inductor performance has been investigated. 30 mins. 600°C thermal annealing performed to have ~7.4% electrical resistivity reduction of Cu film won't result in any inductance variance of on-chip spiral inductor that made of the same Cu. For a total of 18 3.5-circles on-chip spiral inductors, the inductance variance before and after the thermal anneal only ranges from -2.25% to 0.41%. Meanwhile, the resonant frequency associated with the inductance variance also changes from -8.22% to 1.68%. According to hypothesis test statistical method, it shows that these variances are not correlated which can be attributed to experimental variation and there is, in fact, no thermal annealing effect on the inductor performance. The results also indicate that the electrical conductivity is independent of the inductance of on-chip spiral inductor which is matched with the prediction of Greenhouse model but totally contradicts with the model proposed by Chen et al..

誌謝

說到感謝，這一路上我要感謝的人實在太多，首先要感謝我的指導教授鄭裕庭老師，在我實驗遇到問題時他總是能給予我適時的意見，因為他我又成長了不少，不管是學習上或是態度上。另外，博班的兩位學長，陳建章雖然他常嘻嘻哈哈看起來一臉宅樣，但是就像是一位認真於理論的研究者，遇到奇特的現象總是去想辦法解釋它，另一位博班的學長是趙子元，他苦幹的拼勁是我們 MIL 實驗室之冠，在實驗與分析上給我不少的幫助。實驗室的其他同仁也感謝你們，因為我們一起成長一起努力，可愛的濬誠，努力的睿婉，總是在實驗室高歌的任凱，用功的小陸，很帥氣的茄子，期待愛情的阿昌，安靜的瑋廷，和有氣質的家瑋，當然還有為我們排除萬難的筱筑。謝謝你們，因為你們我的碩士兩年變的更加精采。

很早就獨立的我，從大學開始就開始自給自足，甚至能給家裡人一點幫助，這都得感謝我父母給我的態度與教導。最後感謝陪伴我快十年的女友，謝謝妳的鼓勵和支持，伴我度過了許多難關與挫折。

賴文駿

2007.7.18

Contents

摘要……..…….....……i

Abstract…….....ii

誌謝……iii

Content……. iv

Figure Captions…….....v

Table Captions…… … … … …….. vi

Content

Chapter 1 Introduction

1.1 Overview ……..…….1

1.2 Thesis Organization……..…….....3

Chapter 2 Experimental Design and Fabrication Process

2.1 Introduction……..4

2.2 Fabrication Process……6

2.2.1 Introduction……...6

2.2.2 The Surface Inductor Process……..7

2.3 Annealing Principle…….……10

Chapter 3 Resistivity Measurement and Annealing Process

3.1 Resistivity Measurement……12

3.2 Annealing Process……15

Chapter 4 Experimental Results

4.1 Resistivity Measurement Result…… ……..……..17

4.2 Inductance Measurement Results…….……20

Chapter 5 Discussions

5.1 The Investigation of Self-resonant Frequency and Inductance of Spiral Inductor……...……27

5.2 Discuss From Greenhouse's Model of Spiral Inductor……32

5.3 Discuss From C. C. Chen's Model of Spiral Inductor…….....33

Chapter 6 Summary and Future Works

6.1 Summary…….……35

6.2Future Work……35

6.3Reference……36

Vita and Publication…….....…..……38

Figure Captions

Chapter 2

Fig.1 4-points probe structure and spiral inductor…...…….……..…….5

Fig.2 The layout of the micro machined inductor.……6

Fig.3 The surface process flow of cross-membrane type inductor.…….8

Fig.4 Grain growth by annealing……10

Fig.5 Grain growth and electron scattering……11

Chapter 3

Fig.6 Shape parameter of 4 -points probing structure in detail.……13

Fig.7 The top view of a spiral inductor and 4 -points probing structure……14

Fig.8 Current and voltage on 4 -points probing structure.……14

Fig.9 Relations between heating time and temperature……..……16

Chapter 4

Fig.10 Resistivity rate of change after annealed……...…17

Fig.11 Relations between current and voltage..……18

Fig.12 Inductance measurement flow……...…..21

Fig.13 Sample1, 4.5turns inductance of a spiral inductor…….22

Fig.14 Sample2, 4.5turns inductance of a spiral inductor……..22

Fig.15 Sample3, 4.5turns inductance of a spiral inductor…….23

Fig.16 Sample4, 3.5turns inductance of a spiral inductor…….24

Fig.17 Sample5, 3.5turns inductance of a spiral inductor…….24

Fig.18 Sample6, 3.5turns inductance of a spiral inductor…….25

Fig.19 Sample7, 2.5turns inductance of a spiral inductor…….26

Fig.20 Sample8, 2.5turns inductance of a spiral inductor…….26

Chapter 5

Fig.21. 2 turns rectangular planar coil..……32

Table Captions

Chapter 4

TABLE Ⅰ Resistivity measurement result……...…19

TABLE II The inductance rate of change after annealing for 4.5 turns spiral inductors.....23

TABLE III The inductance rate of change after annealing for 3.5 turns spiral inductors.....25

TABLE IV The inductance rate of change after annealing for 2.5 turns spiral inductors.....26

Chapter 5

TABLE V Self-resonant frequency of spiral inductors..... 27

TABLE VI Inductance of spiral inductors..... 28

TABLE VII The parameter for statistics of self-resonant..... 29

TABLE VIII The parameter for statistics of inductance..... 30

TABLE IX Percentiles of the *t* distribution..... 31

Chapter 1 Introduction

1.1 Overview

. In comparison with conventional Al metal, Cu has the characteristics of lower electrical resistivity and higher activation energy of electromigration to ensure better signal integrity and data bandwidth, and longer interconnect life time for the next generation IC [1, 2]. Since the 130 nm-node and beyond [3], Cu interconnecting technology has been the major BEOL (Back-End-of-The-Line) process in CMOS VLSI fabrication. Thus, the investigation related to Cu interconnects have become an important research topic in the technology development of the next generation VLSI, such as developing new low-k dielectric materials, diffusion barrier materials, nanocrystalline copper films…etc..

Cu annealing is a critical process step in the fabrication of Cu interconnects. It provides a way to further reduce the resistivity of Cu but also a way to enhance interconnect reliability [1, 4, 5]. However, the annealing temperature could range from 150 to 400°C. Cu grain growing and surface smoothing controlled by different annealing temperature will result in a distinct material characteristic that significantly affect the electrical performance and reliability of Cu interconnects. For instance, about 400°C annealing temperature differences will cause about 13% resistivity change of Cu film due to 190% grain size increase. [6]

Recent progress in the development of CMOS technology has enabled the realization of a signal chip solution for a microsystem circuitry fabrication where mixed-signal components can be fully integrated as a form of SOC (System-on-a-Chip) [7]. Such a microsystem can be expected with a small form factor, low power consumption, and excellent system performance [8]. Meanwhile, in a CMOS RFIC, on-chip spiral inductor is a critical passive component for circuit impedance matching, voltage biasing, signal resonating and filtering…etc. and it is generally made of the BEOL materials, i.e. Al or Cu interconnects. In 2005, Chen et al. [9] has proposed a closed-form integral which could well predict the

inductance and self resonant frequency of a micromachined spiral inductor. The integral also revealed the relations between the inductor characteristics and the geometric factors and material properties of inductor. Since the BEOL processes will be different in different CMOS technology node and foundry, it will be critical to circuit designers and process engineers to understand the relation between the resistivity of inductor material and .the inductance of the inductor while they are developing a wireless microsystem SOC. Thus, in this paper, the aforementioned relation is studied based on the inductance measurement of rectangular on-chip spiral inductors before and after 600°C post-annealing process. The inductors are designed and fabricated on a 4' silicon wafer by three layer electroplated copper process. A 4 point probe testing pattern is also designed and fabricated to monitor the resistivity change of Cu.

1.2 Thesis Organization

Experimental design is shown in Chapter 2, described the experimental construction and the principle, including the measurement resistance structure and the spiral inductor structure, and describe the annealing the environmental condition. In the chapter 3, it tell us how measure resistivity in this experimental and annealing process. And the experimental results will show in the chapter 4, including resistivity and inductance of spiral inductors. In the chapter 5, we use statistics method and Greenhouse's model and C. C. Chen's model to discuss experimental results. Finally, the summary and future works are presented in the chapter 6.

Chapter 2 Experimental Design and Fabrication Process

2.1 Introduction

In this experimental, we have designed rectangular spiral inductors and 4-points probe structures as shown in Fig.1 to characterize the inductance of spiral inductor and the electrical resistivity of the Cu film that was used to make the inductor. Firstly, we measure the values of inductance and the resistivity on a total of 21 inductors and 6 probe structures. After thermal annealing, we measure the values of inductance and the resistance on the same devices again to observe the correlation.

The annealing process, we used Backend Vacuum Annealing Furnace to anneal the chip, which can carry on the high vacuum heating at 600℃, and the pressure can to 10^{-6} torr below. This furnace caused the chip to reduce the oxidized probability in the annealing process.

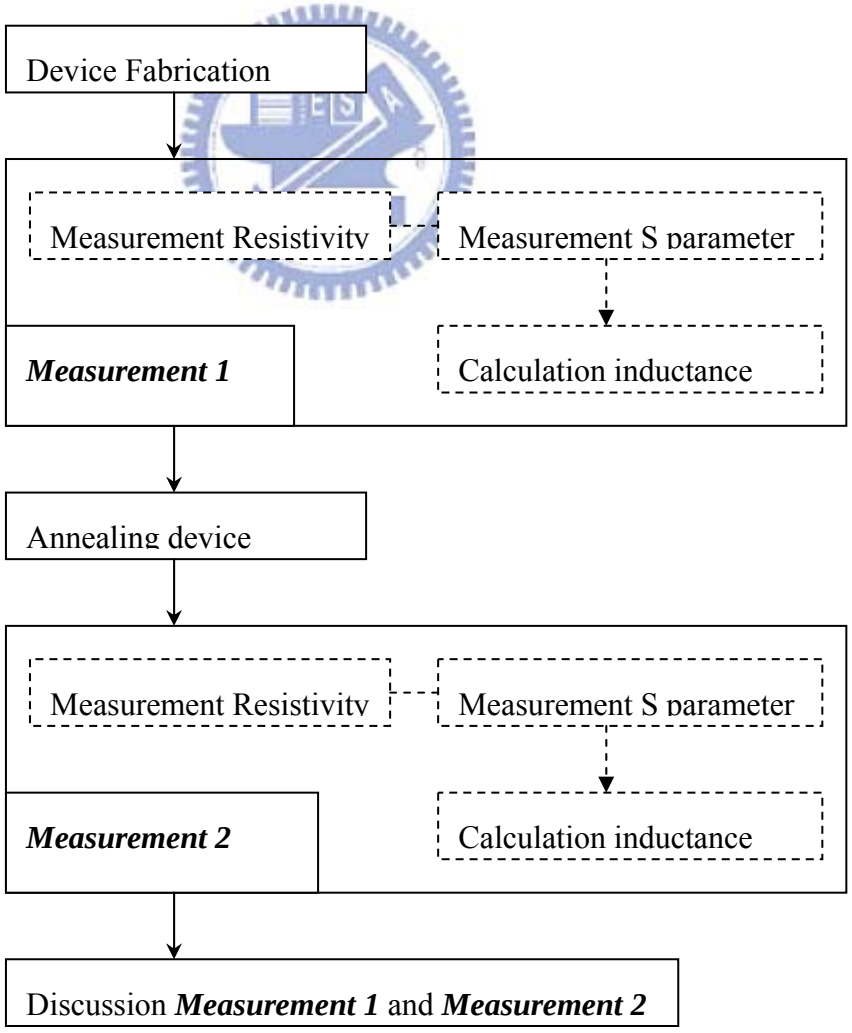

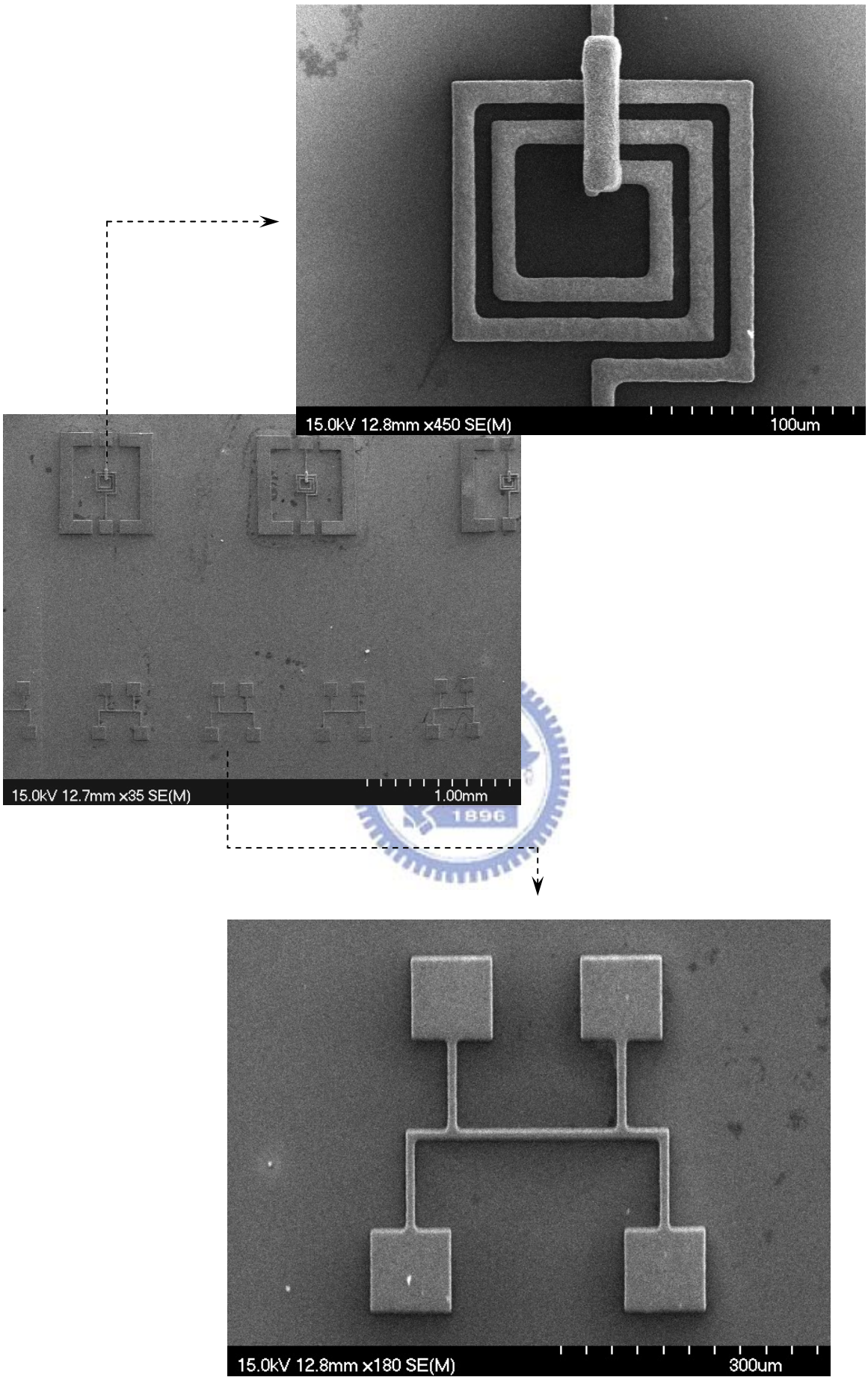

Fig.1. 4-points probe structure and spiral inductor

2.2 Fabrication Process

2.2.1 Introduction

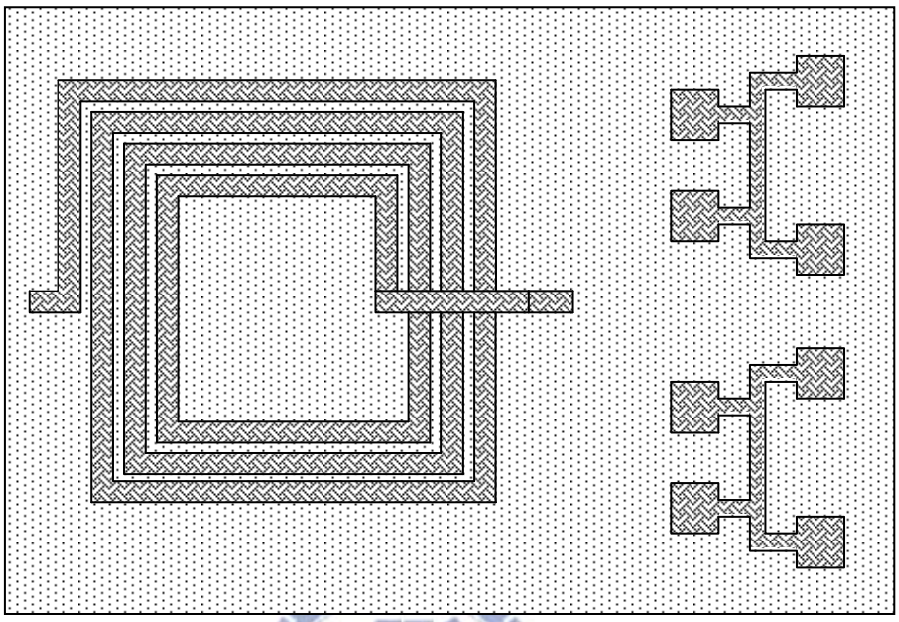

(a) The top view of micro machined inductor.

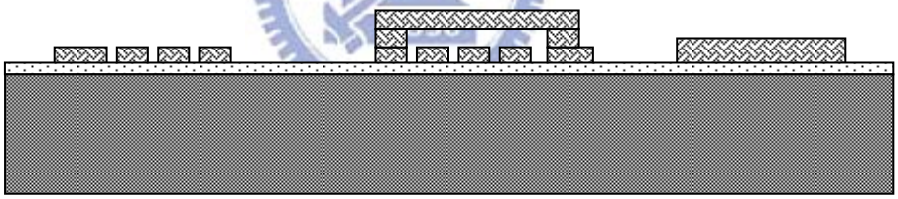

(b) The cross view of micro machined inductor

Fig2. The layout of the micro machined inductor.

As illustrated in Fig2, the main structure of the spiral inductor is consisted of 3.5 turn's electroplated copper coil with the thickness 5μm, the width 10μm, the spacing 5μm and the outset diameters of 300μm and the air-bridge with thickness 5μm and height 15μm.

2.2.2 The Surface Inductor Process

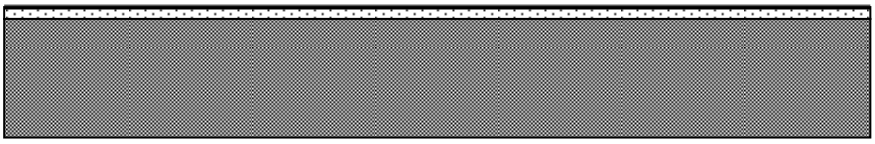

(a) Thermal oxide SiO_2 and Ti/Cu (100A/1200A) seed/adhesion layer deposition.

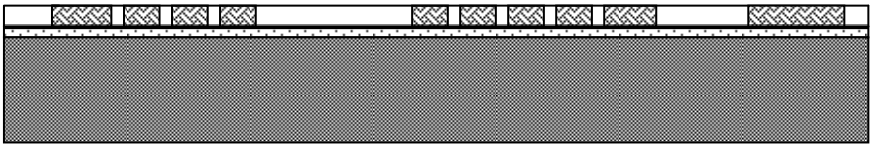

(b) The first copper plating for the coil part of the inductor.

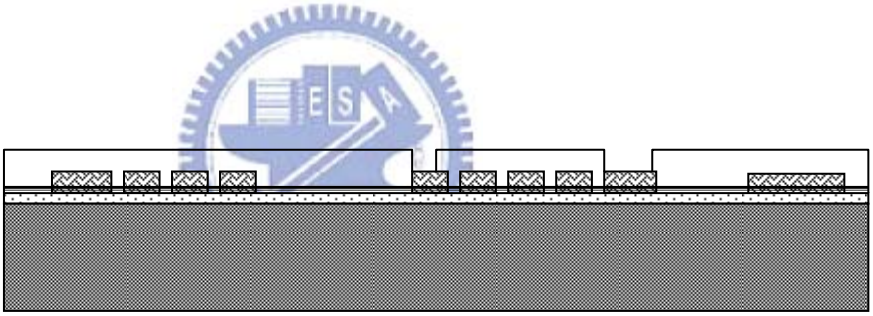

(c) The patterned photo-resist to define the via hole.

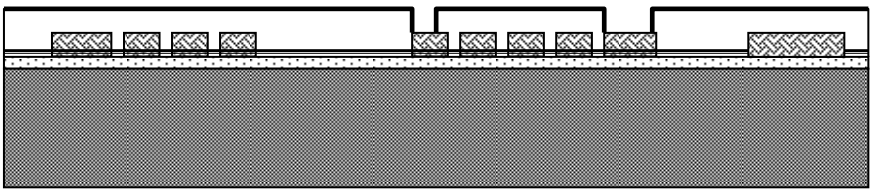

(d) The seed layer of air-bridge deposition for air-bridge via filling.

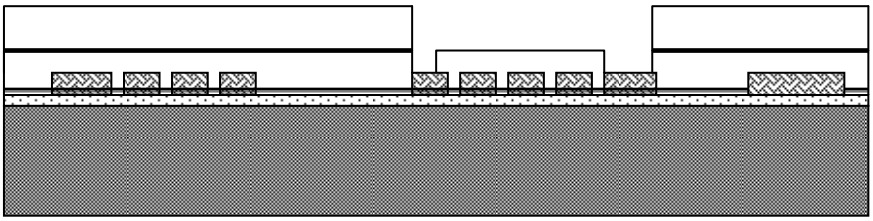

(e) The patterned photo-resist to define the air-bridge.

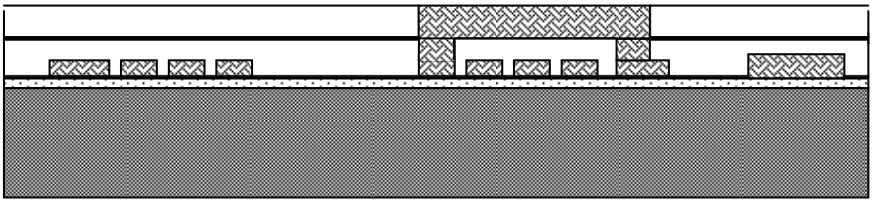

(f) The fabrication of the air-bridge.

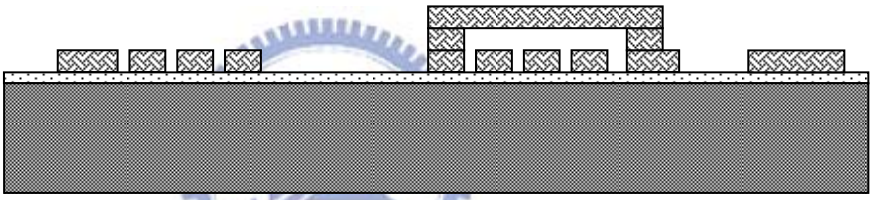

(g) Photo-resist and seed layer

removal.

Fig3. The surface process flow of cross-membrane type inductor.

Fig.3 illustrates the surface micromachined process. It begins with wet oxidation at 1050ºC for 700nm of thermal oxide and sputtered the first thin Ti/Cu (10nm /120nm) adhesion/seed layer onto a p-type silicon substrate as shown in figure (a). Figure (b) shows that then patterned with a 6-7μm thick AZ 4620 photo-resist to define the region for the fabrication of the coil part of the spiral inductor using copper electroplating. After plated the first layer of copper, a 10μm AZ4620 is spin-coated, patterned to define the via hole figure (c), and sputtered with another 100nm copper seed layer on the same substrate as shown in figure (d) for the air-bridge copper via filling. Figure (e) illustrates that, after the seed layer of the via filling, another 10μm AZ4620 is spun onto the plated structure, patterned to define the air-bridge beam, and plated with 5μm copper to form the air bridge as showed in figure (f). Finally, the fabrication of the spiral inductor is done after lift off the underneath copper seed layer and chemically etch away the first seed/adhesion layer using CR-7T as shown in figure (g).

2.3 Annealing Principle

Annealing is refers the material heating to some temperature, and holds that's temperature in the few time. The translation, vibration and rotation of the atom are not intense when low temperature, but intense at high temperature. Atomic movement will cause partial atom suitably rearranges in the annealing process. This process is different along with the annealing temperature and the time, divides into recovery, recrystallization and grain growth three stages.

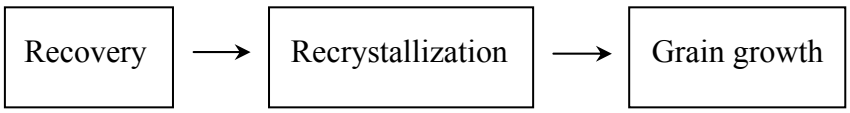

At high temperature, in the atoms will be rearranging by the intense heat movement. There is a grain boundary between the grains including same orientation atoms before annealing process, and the impact of electron scattering from grain boundaries. The atoms belonging different grain will have in order arrangement, causes grain boundaries to vanish gradually. After grain boundaries vanishing, can create the electron scattering place also vanishing. Therefore, resistivity will reduce during annealing process.

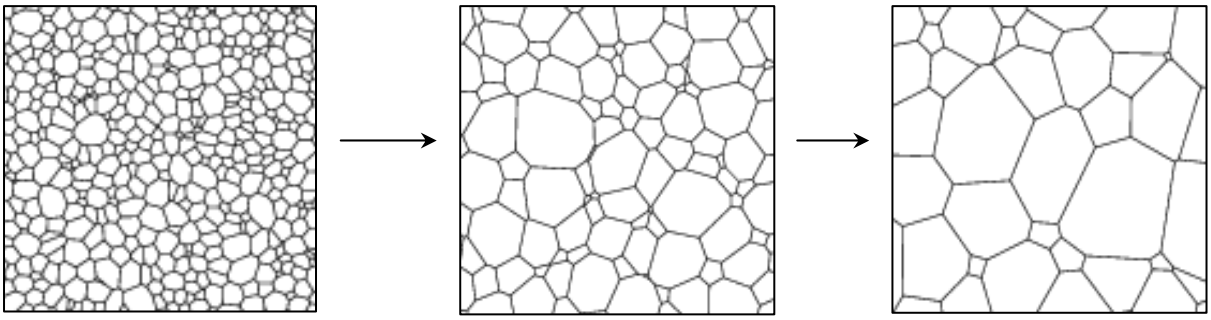

Fig.4. Grain growth by annealing

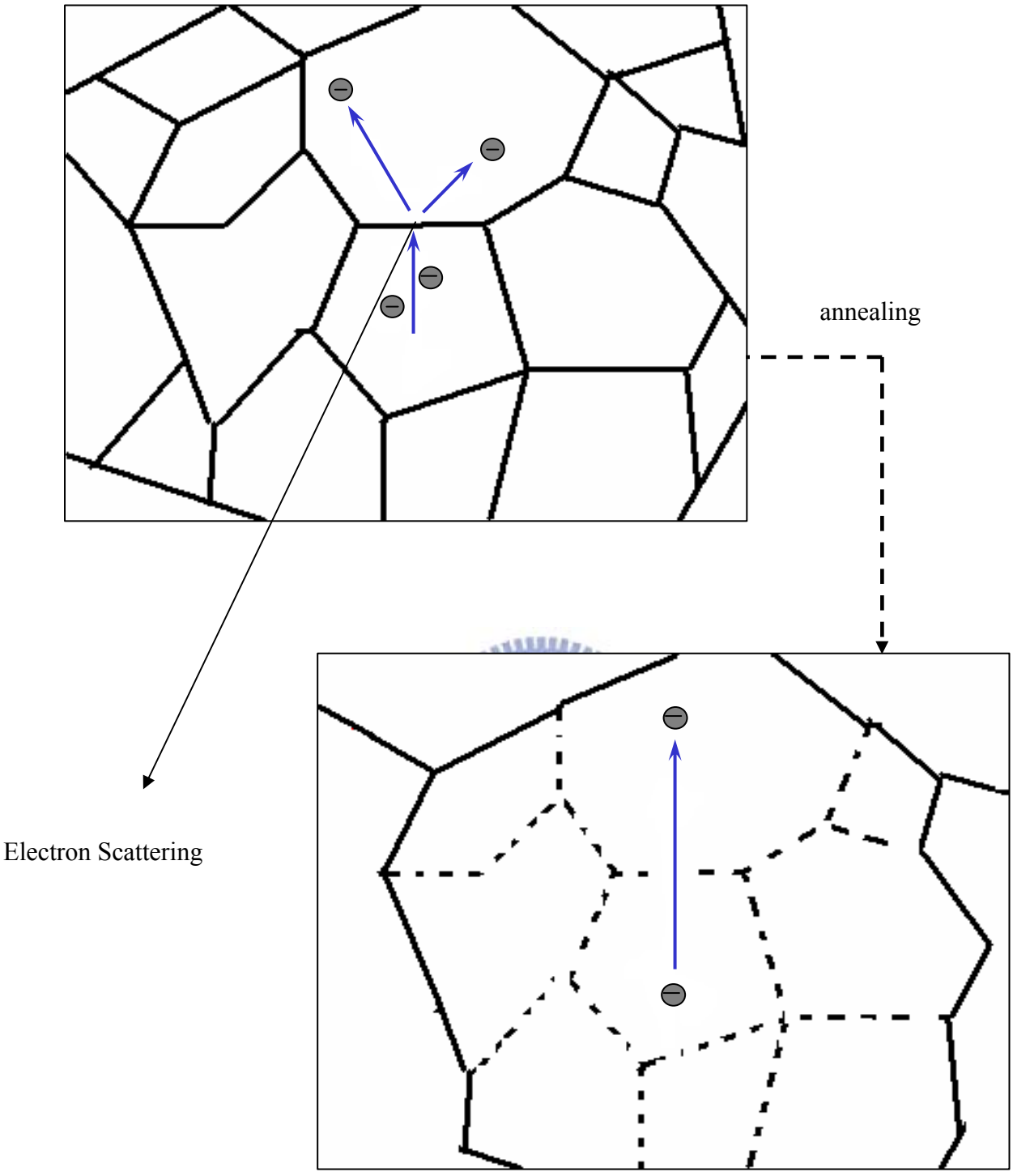

Fig5. Grain growth and electron scattering

Chapter 3 Resistivity Measurement and Annealing Process

3.1 Resistivity Measurement

The calculating resistance method is show as following. We used *HP* 4156B Parameter Analyzer and *Elerbeing* Probe Station to measure voltage (V_1, V_2) along with current (I) change. The current I changed from 100μA to 10mA with 50μA one step, and used formula (1) to calculate resistance R of. 4 point probing structure.

$$R = \frac{V_1 - V_2}{I} \tag{1}$$

$$R = \rho \frac{\ell}{d \times h} \tag{2}$$

where ρ is resisivity of copper, ℓ, d and h are 200 μm, 10 μm, and 5 μm, respectively, as illustrated in Fig6. We use formula (2) to calculate resisivity ρ.

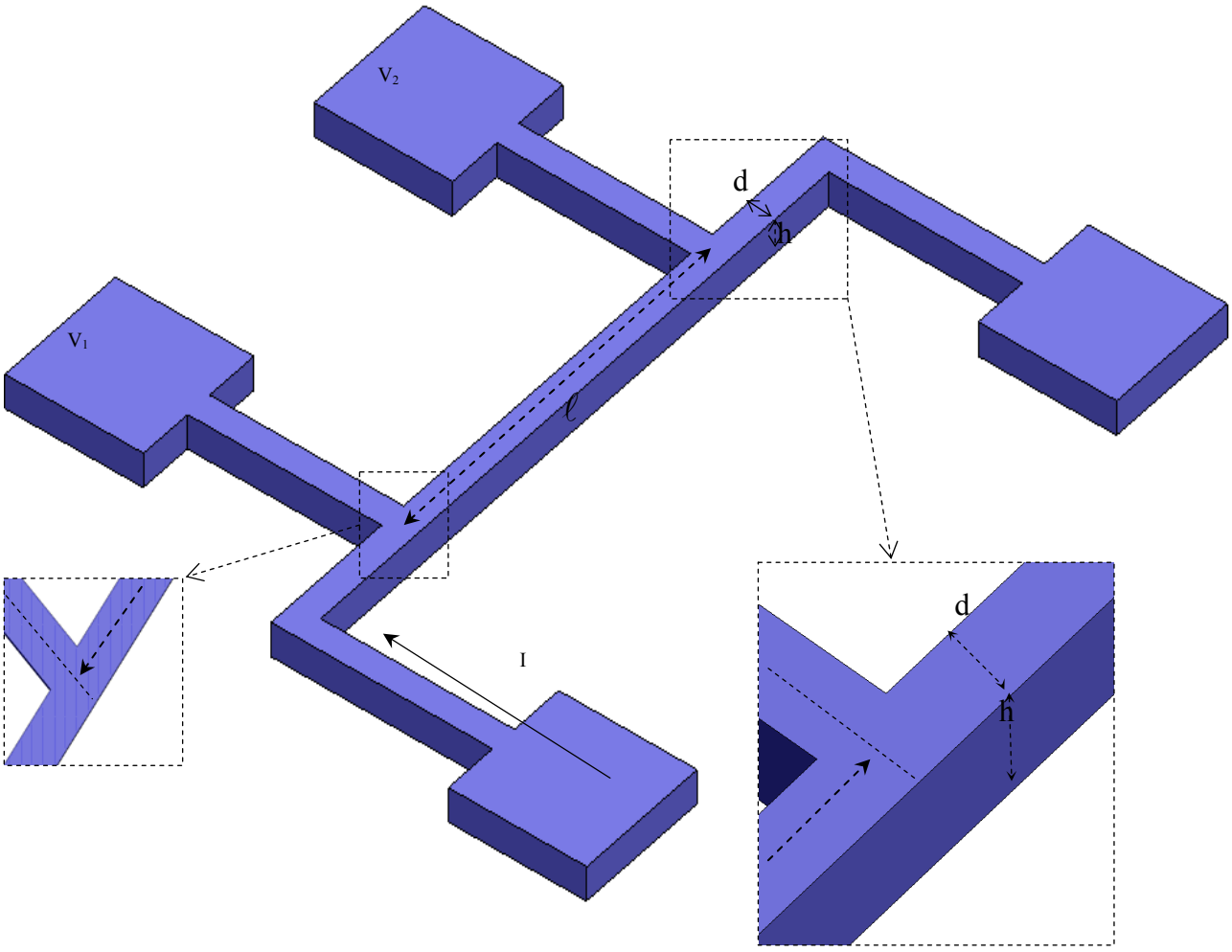

Fig.6. Shape parameter of 4 -points probing structure in detail

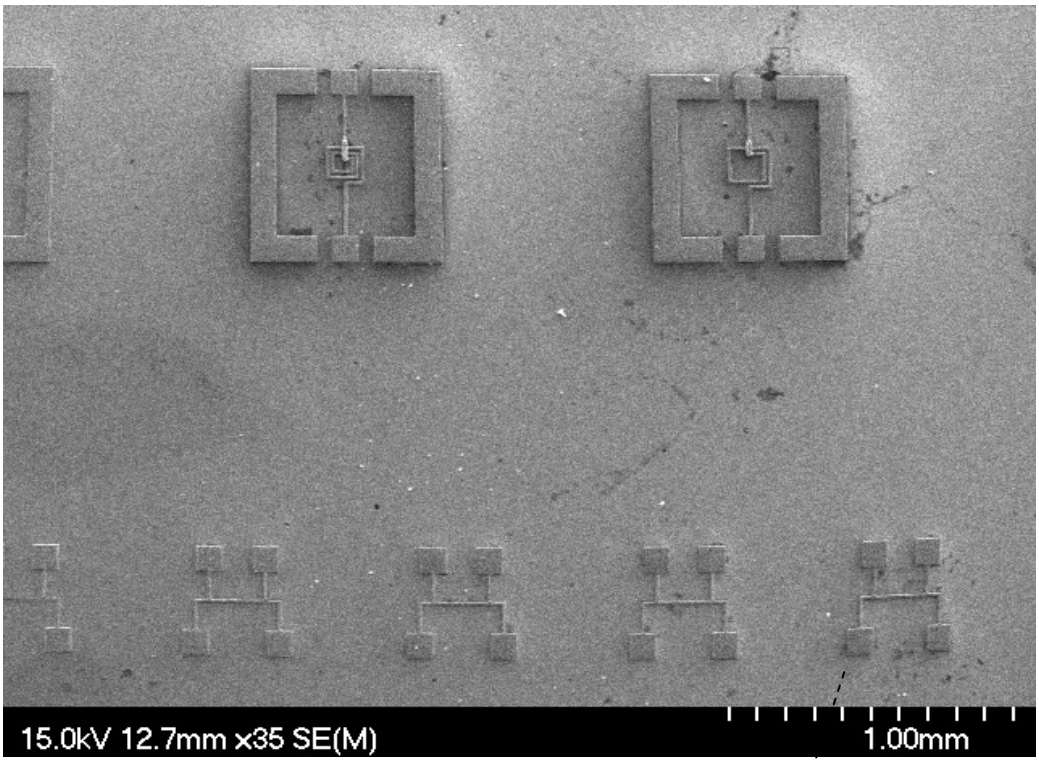

Fig.7.The top view of a spiral inductor and 4 -points probing structure

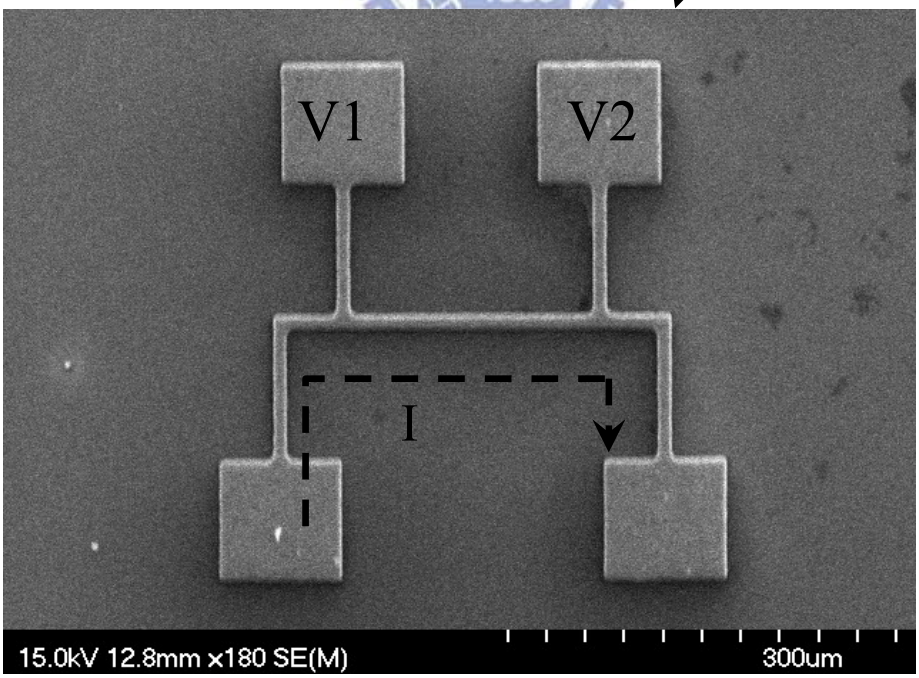

Fig.8. Current and voltage on 4 -points probing structure

3.2 Annealing Process

In our annealing process, we first make temperature increasing to 600℃ and vacuum reach to 10^{-6} torr in the chamber, when the temperature arrives, we put chip in the chamber and heat up 30 minutes. After heating time up, we closed heating under the vacuum state to employ the chip reduce temperature slowly, and temperature relax time about 6 hours, when temperature relax to room temperature, we pull out the chip from the furnace. The heating time is illustrated in Fig.9.

A. Heat the furnace to 600°C
B. Put sample into the chamber
C. Heating 30mins
D. Close heating
E. Waiting temperature to room temperature about 6 hours
F. Put out sample from the chamber

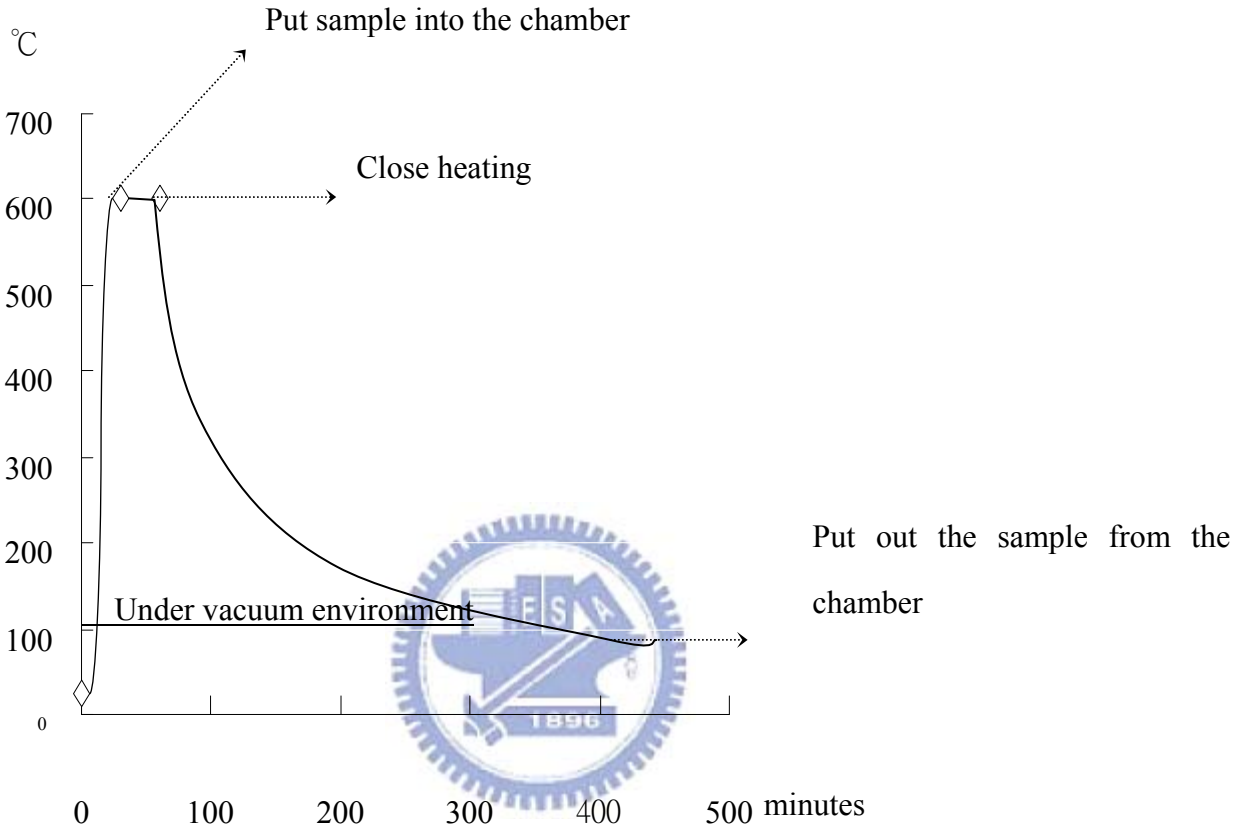

Fig.9. Relations between heating time and temperature

Chapter 4 Experimental Results

4.1 Resistivity Measurement Result

The 4-points probing structure was used for measuring resistance, after annealing, the result is shown as Fig.11. The resistance has decreased by annealing. Fig.10 shows average resistivity change.

As illustrated in Fig.10, we choose 6 samples to calculate its resisivity. The resistivity average reduces 7.40%. The resistivity of samples has show in Table Ⅰ, the measurement resistivities close to 17.2 nΩ-m which the resistivity of copper from [11].

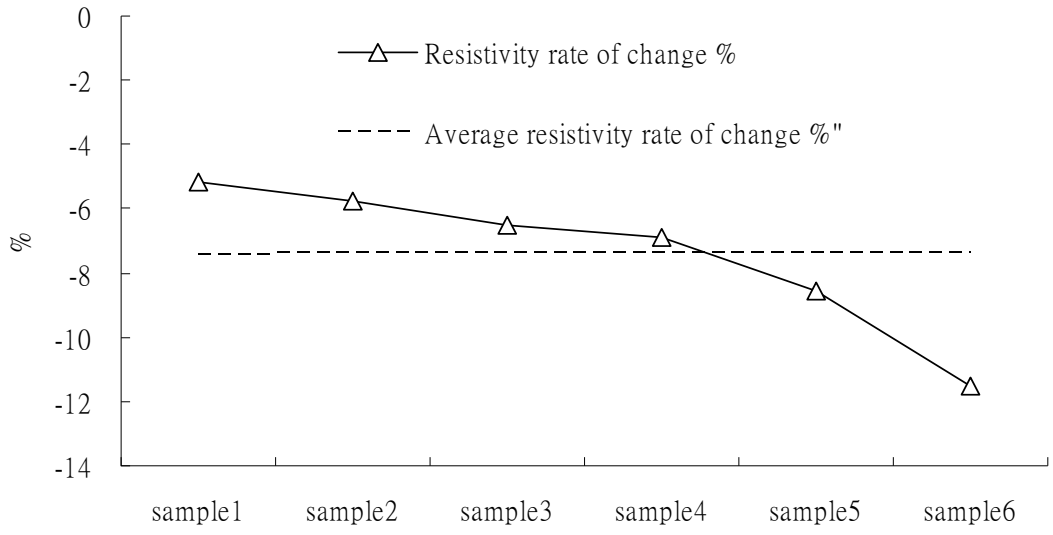

Fig.10. Resistivity rate of change after annealed

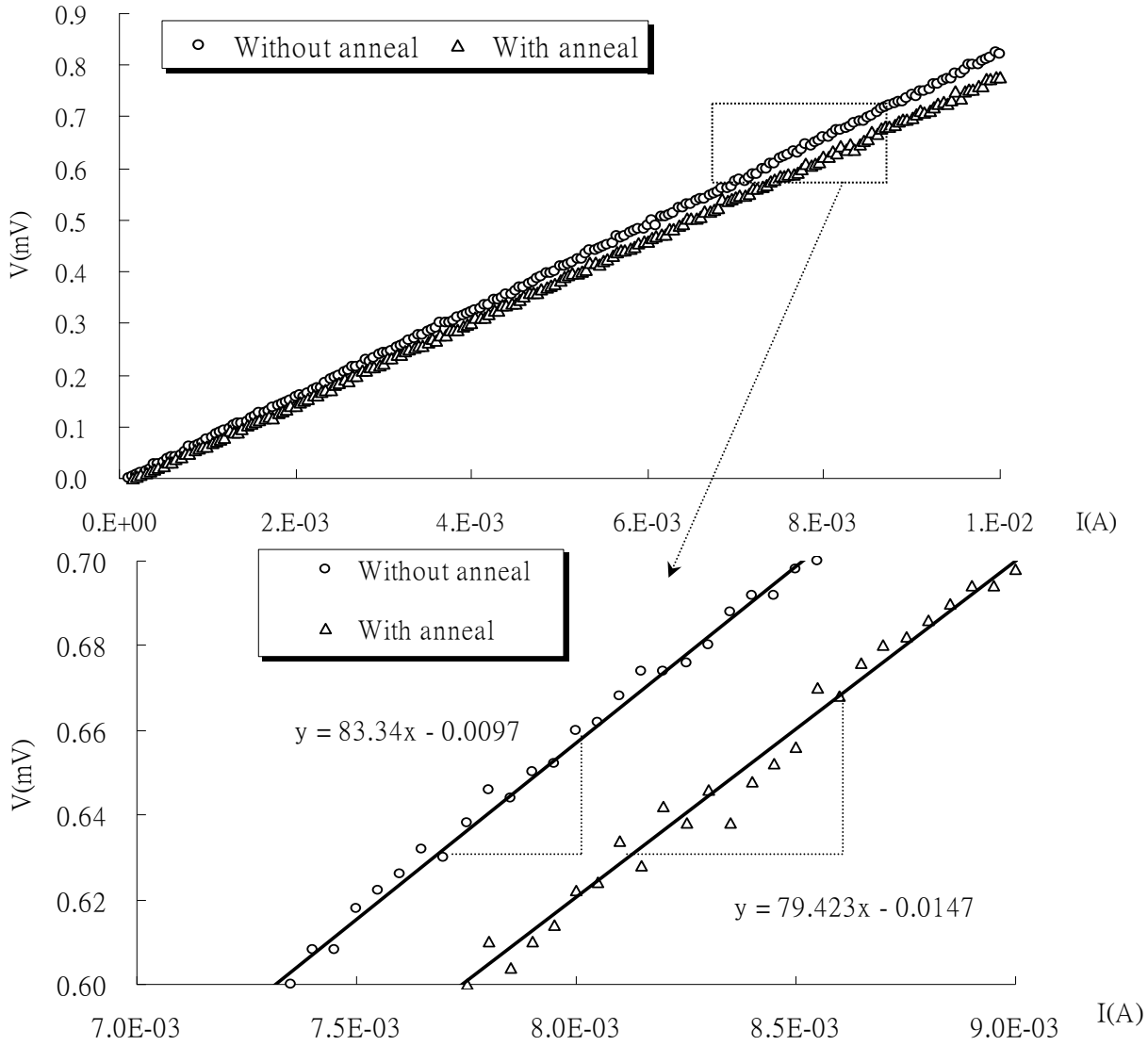

Fig.11. Relations between current and voltage.

TABLE I

Resistivity measurement result

Samples	Resistivity (nΩ-m)	Resistivity annealed (nΩ-m)	Resistivity rate of change (%)
R1	17.94	17.01	-5.19
R2	18.24	17.19	-5.74
R3	20.35	19.02	-6.52
R4	22.05	20.53	-6.87
R5	23.85	21.81	-8.57
R6	25.86	22.88	-11.54

4.2 Inductance Measurement Results

Following figures are inductance of 2.5turns, 3.5turns and 4.5turns spiral inductors, Fig13~15 are 4.5 turns spiral inducts in different place on chip, Fig16~18 are 3.5 turns spiral inducts in different place on chip, Fig19, 20 are 2.5 turns spiral inducts in different place on chip ,and has demonstrated that difference and the error bar. Table Ⅱ, Ⅲ, Ⅳ is point out the resistivity rate of change after annealing at frequency 1GHz, 3GHz, 5GHz. The inductances change small in Fig.13~20, and error bar including ΔL, that is mean that the small change is experiment error.

For the inductance L extract, we select Cascade RF-1 Microwave Probing Station and Agilent E8364B PNA to get the S parameter, and use the following formula (3) to calculate the inductance,

$$L = \frac{\mathrm{Im}\left(\frac{1}{Y_{11}}\right)}{2\pi f} \tag{3}$$

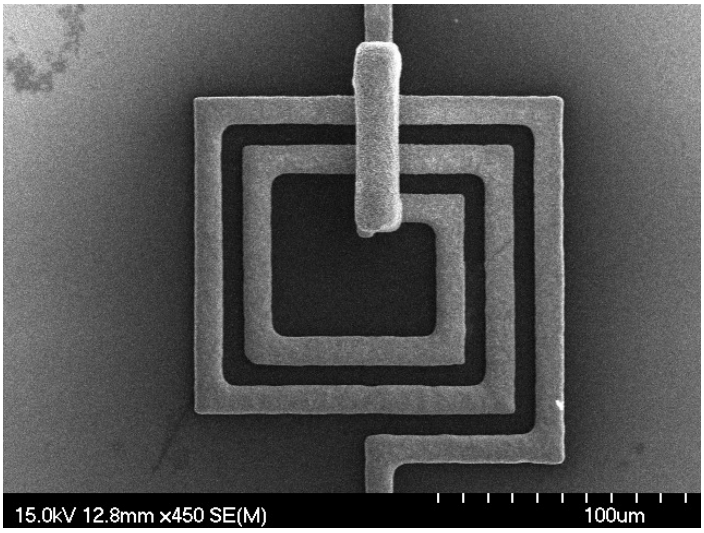

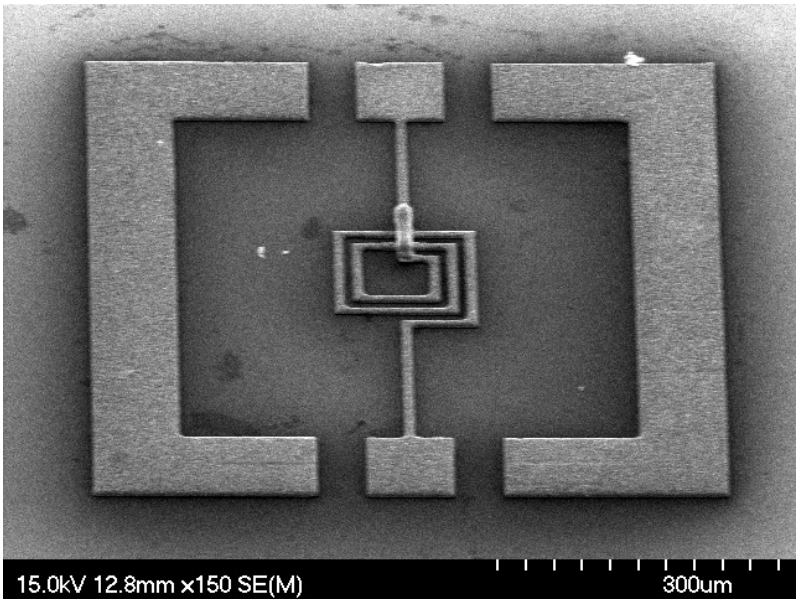

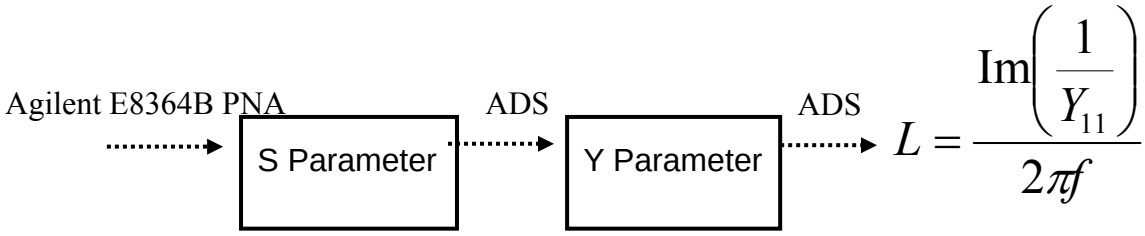

Fig12. Inductance measurement flow

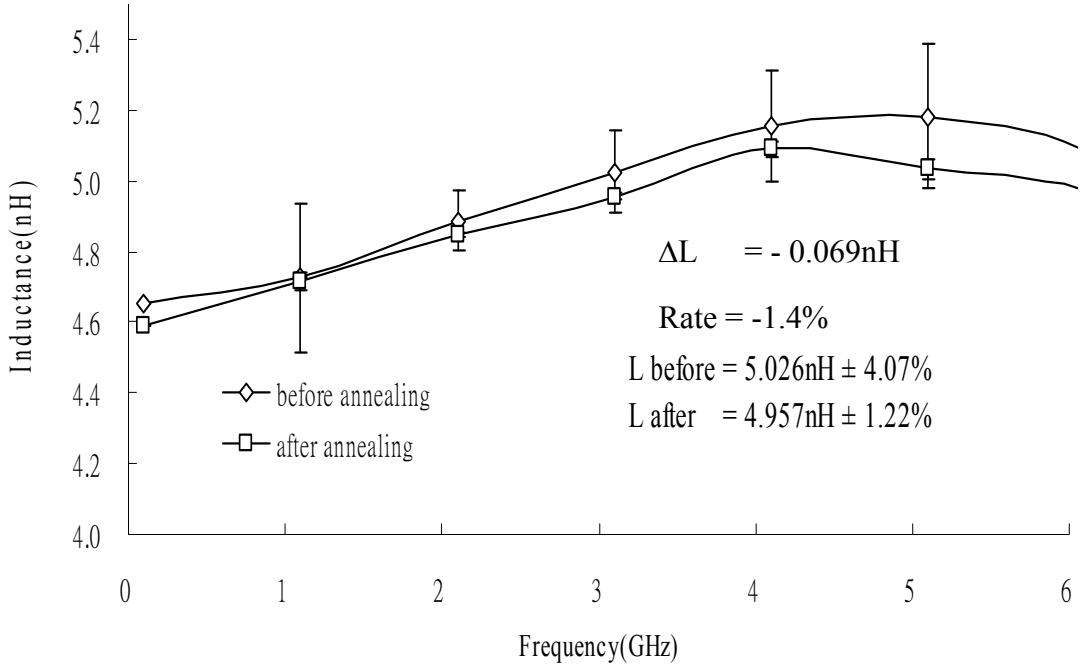

Fig.13. Sample1, 4.5turns inductance of a spiral inductor

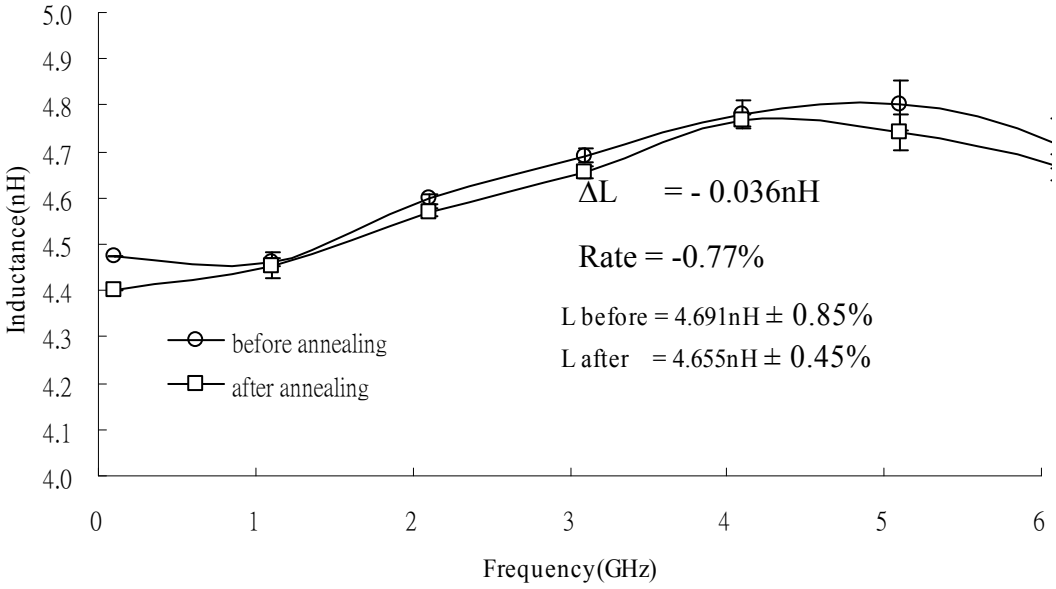

Fig.14. Sample2, 4.5turns inductance of a spiral inductor

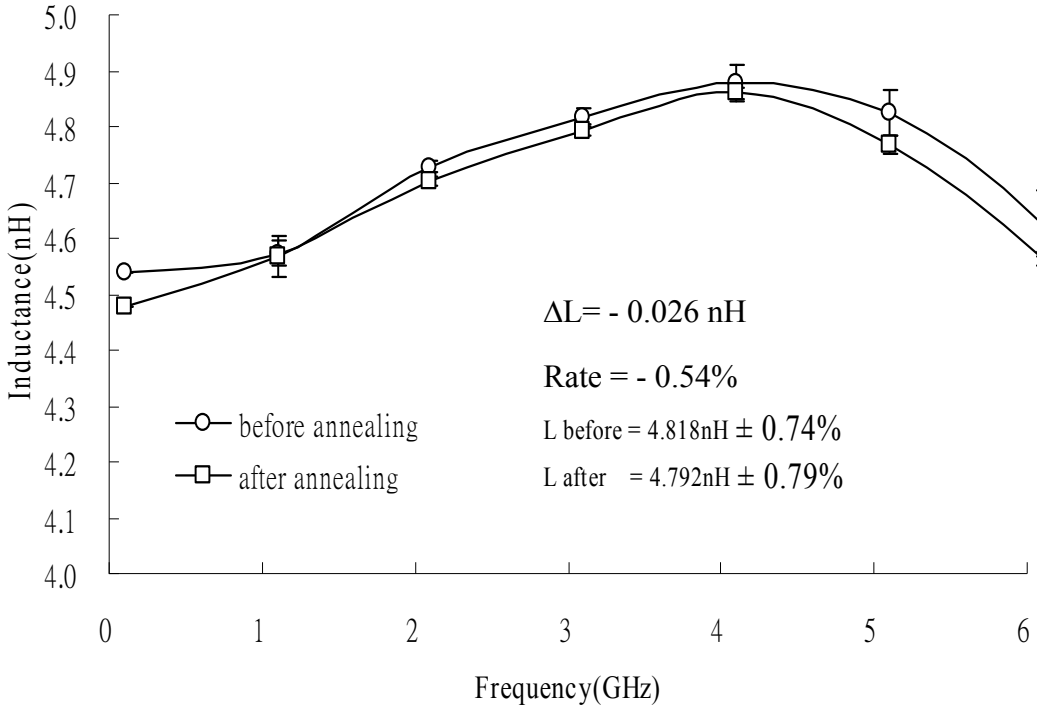

Fig.15. Sample3, 4.5turns inductance of a spiral inductor

TABLE Ⅱ

The inductance rate of change after annealing for 4.5 turns spiral inductors

	Sample1	Sample2	Sample3
1GHz	-0.20%	-0.18%	-0.13%
3GHz	-1.37%	-0.77%	-0.53%
5GHz	-2.90%	-1.23%	-0.12%

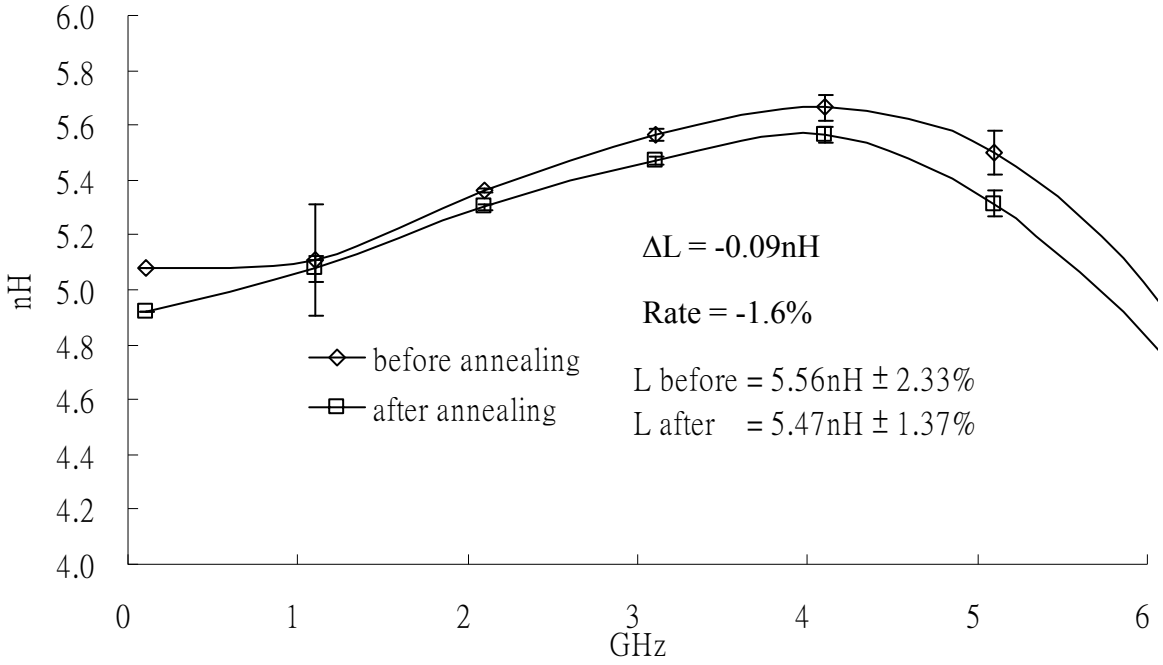

Fig.16. Sample4, 3.5turns inductance of a spiral inductor

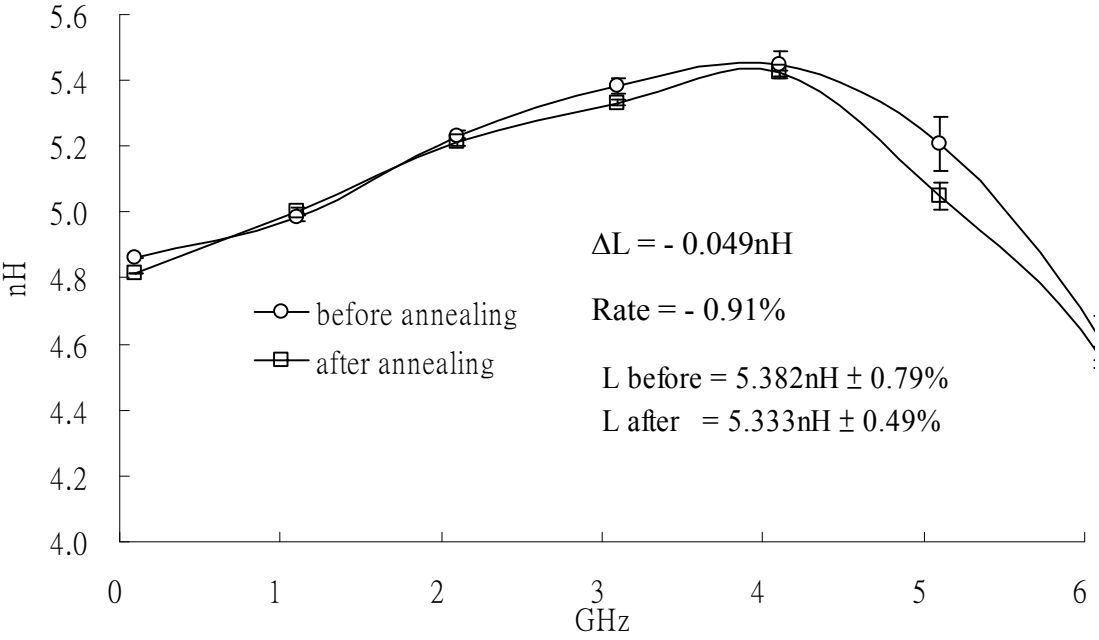

Fig.17. Sample5, 3.5turns inductance of a spiral inductor

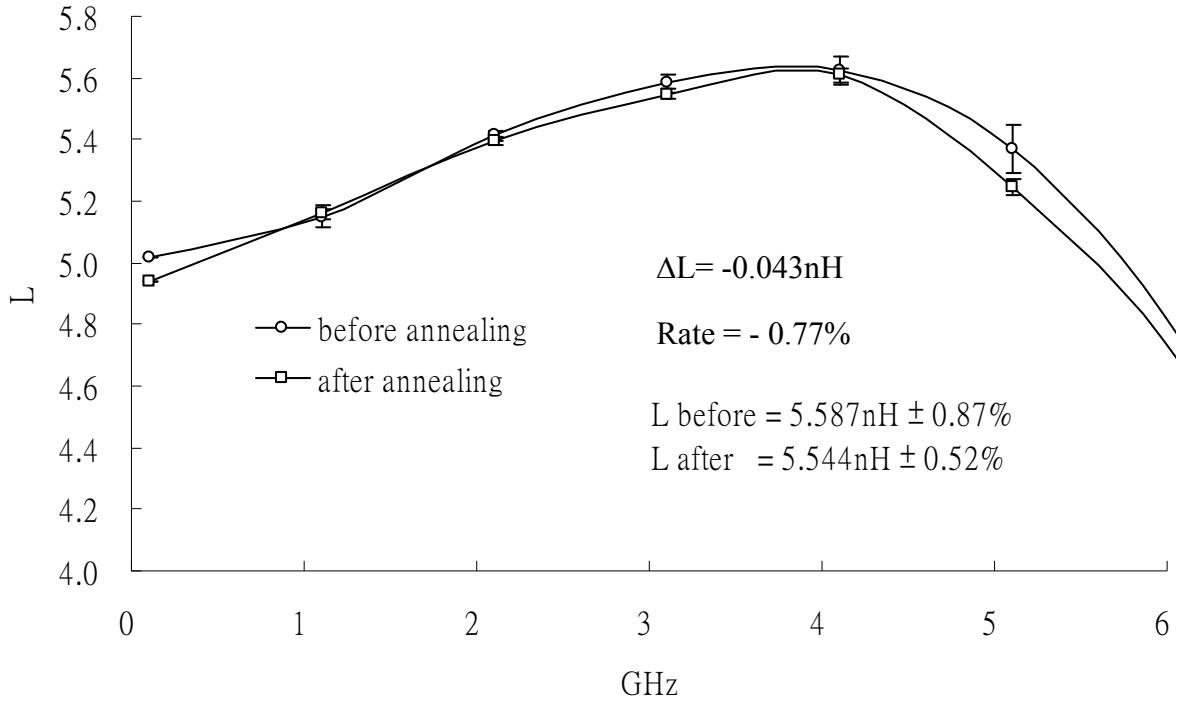

Fig.18. Sample6, 3.5turns inductance of a spiral inductor

TABLE Ⅲ

The inductance rate of change after annealing for 3.5 turns spiral inductors

Rate	Sample4	Sample5	Sample6
1GHz	-0.56%	0.30%	0.17%
3GHz	-1.71%	-0.90%	-0.76%
5GHz	-3.35%	-3.08%	-2.34%

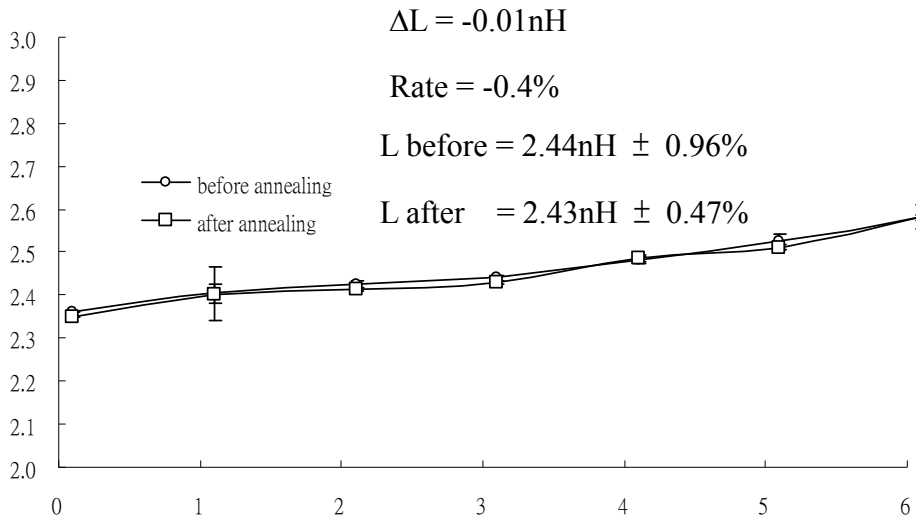

Fig.19. Sample7, 2.5turns inductance of a spiral inductor

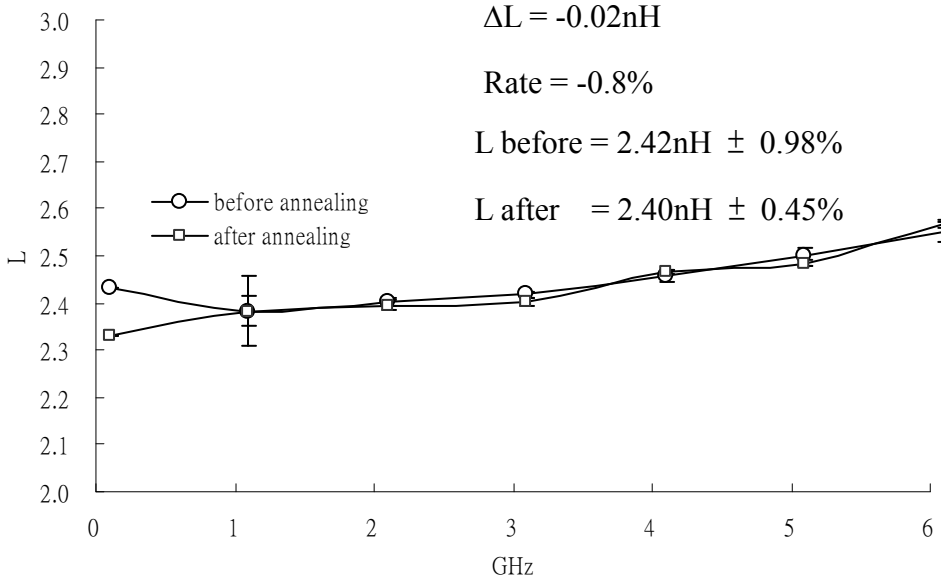

Fig.20. Sample8, 2.5turns inductance of a spiral inductor

TABLE Ⅳ

The inductance rate of change after annealing for 2.5 turns spiral inductors

Rate	Sample7	Sample8
1GHz	-0.07%	0.002%
3GHz	-0.46%	-0.63%
5GHz	-0.53%	-0.57%

Chapter 5 Discussions

5.1 The Investigation of Self-resonant Frequency and Inductance of Spiral Inductor

Table Ⅴ and TableⅥ show that self-resonant and inductance of spiral inductors, where A1~A4, B1~B4, C1 and C2 are 3.5 turns spiral inductors, A1~A4 with the outset diameters of 300μm, the spacing 5μm, the thickness 5μm, the width 15μm, B1~B4 with the outset diameters of 250μm, the spacing 5μm, the thickness 5μm, the width 15μm, C1 and C2 with the outset diameters of 230μm, the spacing 5μm, the thickness 5μm, the width 15μm, ω_r is self-resonant of spiral inductor and L is inductance of spiral inductor.

$$\omega_r = \frac{1}{\sqrt{LC}} \tag{4}$$

TABLE Ⅴ

Self-resonant frequency of spiral inductors

	ω_r (GHz)	ω_r (annealed)(GHz)	$\Delta\omega_r$ (GHz)	$\Delta\omega_r / \omega_r$ %
A1	11.68	10.72	-0.96	-8.22
A2	11.82	11.78	-0.04	-0.34
A3	11.57	11.48	-0.09	-0.78
A4	11.61	11.54	-0.07	-0.60
B1	16.32	16.33	0.01	0.06
B2	16.19	16.17	-0.02	-0.12
B3	16.13	16.17	0.04	0.25
B4	16.21	16.32	0.11	0.68
C1	19.62	19.95	0.33	1.68
C2	19.16	19.09	-0.07	-0.37

TABLE Ⅵ

Inductance of spiral inductors

	L (nH)	L (annealed)(nH)	ΔL (nH)	$\Delta L / L$ %
A1	5.03	5	-0.03	-0.60
A2	4.89	4.91	0.02	0.41
A3	4.91	4.91	0	0.00
A4	5.06	5.07	0.01	0.20
B1	3.56	3.48	-0.08	-2.25
B2	3.55	3.55	0	0.00
B3	3.55	3.56	0.01	0.28
B4	3.65	3.65	0	0.00
C1	3.02	3.03	0.01	0.33
C2	3.01	3.01	0	0.00

From formula (4), assume capacity C is constant, if self-resonant increase then inductance of spiral inductor would decrease simultaneously. But it is not obvious to find tendency between inductance and resistivity. So we use hypothesis test of statistics method to discuss it as shown in Table Ⅶ and Table Ⅷ.

TABLE Ⅶ

The parameter for statistics of self-resonant

	ω_r (GHz)	ω_r (annealed)(GHz)	$\Delta\omega_r$ (GHz)
A1	11.68	10.72	-0.96
A2	11.82	11.78	-0.04
A3	11.57	11.48	-0.09
A4	11.61	11.54	-0.07
B1	16.32	16.33	0.01
B2	16.19	16.17	-0.02
B3	16.13	16.17	0.04
B4	16.21	16.32	0.11
C1	19.62	19.95	0.33
C2	19.16	19.09	-0.07
$\overline{D}$		=0.08	
S		=0.334	
$s_{\overline{D}}$		=0.106	
t		=0.719	
df		=9	

TABLE Ⅷ

The parameter for statistics of inductance

	L (nH)	L (annealed)(nH)	ΔL (nH)
A1	5.03	5	-0.03
A2	4.89	4.91	0.02
A3	4.91	4.91	0
A4	5.06	5.07	0.01
B1	3.56	3.48	-0.08
B2	3.55	3.55	0
B3	3.55	3.56	0.01
B4	3.65	3.65	0
C1	3.02	3.03	0.01
C2	3.01	3.01	0
$\overline{D}$		=0.01	
S		=0.029	
$s_{\overline{D}}$		=0.009	
t		=0.651	
df		=9	

Symbol definition:

1. $\Delta\omega_r$ represents $\omega_r - \omega_r$ (annealed).
2. ΔL represents $L - L$ (annealed).
3. $\overline{D}$ represents mean of $\Delta\omega_r$ or ΔL.
4. S represents standard dispersion of $\Delta\omega_r$ or ΔL as (5).
5. df represents number of cells – number of independent parameters fitted – 1.
6. t represents as (7) and t distribution show as TABLE Ⅸ.

7. $s_{\bar{D}}$ represents estimated standard error as (6).

$$S = \sqrt{\frac{\sum \left(x - \bar{x}\right)^2}{n-1}} \tag{5}$$

where x is sample and $\bar{x}$ is sample mean, n is numbers of samples.

$$S_{\bar{D}} = \sqrt{\frac{S^2}{n}} \tag{6}$$

$$t = \frac{\overline{D}}{S_{\bar{D}}} \tag{7}$$

For self-resonant in Table Ⅶ, The null hypothesis Ho:μd ≦ 0 (not reduced), P(t(9) > 0.719) > 0.2, so that we do not reject Ho; P(t(9) < 0.719) < 0.3, so that we reject Ho.

For inductance in Table Ⅷ, The null hypothesis Ho:μd ≦ 0 (not reduced), P(t(9) > 0.651) > 0.2, so that we do not reject Ho; P(t(9) < 0.651) < 0.3, so that we reject Ho.

The hypothesis test has shown that if want to believe the self-resonant and inductance of spiral inductor have the reduced tendency, the error probability would be situated between 20% and 30%. This statistics result show that self-resonant decrease and inductance decrease, can not explain from formula (8). The inductance change thought is the experimental error.

TABLE Ⅸ

Percentiles of the *t* distribution

df	$t_{.60}$	$t_{.70}$	$t_{.80}$	$t_{.90}$	$t_{.95}$
8	0.262	0.546	0.889	1.397	1.860
9	0.261	0.543	0.883	1.383	1.833
10	0.260	0.542	0.879	1.372	1.812

5.2 Discuss From Greenhouse's Model of Spiral Inductor

Greenhouse's model [12] proposes one computation inductance of a spiral rectangular inductor. In order to simplify computation, the spiral rectangular inductor in [12] has show as illustrated in Fig.21. L_0 is the sum of the self-inductances of all the straight segments, M_+ is the sum of the positive mutual inductances, M_- is the sum of the negative mutual inductances and L_T is total inductance. Clearly, the resistivity is impendent of total inductance.

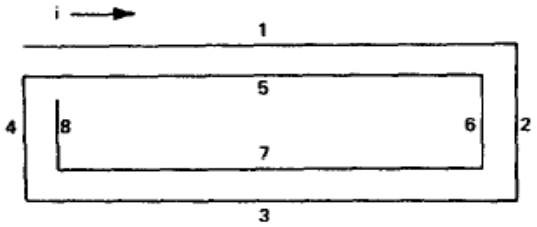

Fig.21. 2 turns rectangular planar coil.

Then inductance of Fig.17 is

$$L_T = L_0 + M_+ - M_- \tag{8}$$

Where

$$L_0 = \sum_{i=1}^{13} L_i$$

$$M_- = 2\left(M_{1,7} + M_{1,3} + M_{5,7} + M_{5,3} + M_{2,8} + M_{2,4} + M_{6,8} + M_{6,4}\right)$$

$$M_+ = 2\left(M_{1,5} + M_{2,6} + M_{3,7} + M_{4,8}\right)$$

5.3 Discuss From C. C. Chen's Model of Spiral Inductor

In 2005, Chen et al. [9], we can obtain

$$L \equiv \frac{\int \overrightarrow{H^*} \cdot \vec{B} dv}{I^2} \approx \mu_0 d(1 + \Re e\chi(\omega)) \tag{9}$$

Where

$$d = \frac{n_e{}^2 l_{total}{}^3 \hbar \omega_r}{2\pi \sigma_0{}^2 An} \left[\exp\left(\frac{\hbar(\omega - \omega_r)}{k_B T} \right) + 1 \right]^{-1} \tag{10}$$

where A is the cross section area, k_B is the Boltzmann's costant, and T is absolute temperature, n_e is the free electron density, $\hbar$ is the Planck's constant, ω_r is the realistic Self-resonant frequency, σ_0 is the dc conductivity of metal, l_{total} is total length of inductor and the real of the susceptibility $\chi(\omega)$ detailed elaboration in [9].By (9) and (10), if assume that every parameters except conductivity σ_0 are constant, then the inductance has inverse with conductivity square ($L \propto \frac{1}{\sigma_0{}^2}$), also may explain with $L \propto \rho^2$, where $\rho \propto \frac{1}{\sigma_0}$.

In our experiment, resistivity reduces 7.40% by annealing.

Let $L_1 \propto \rho_1{}^2$ and $L_2 \propto \rho_2{}^2 (L_2 = L_1 + \Delta L, \rho_2 = \rho_1 + \Delta\rho)$, where L_1 , L_2 , ρ_1 , ρ_2 and $\Delta\rho$ are inductance before annealing, inductance after annealing, resistivity before annealing and resistivity after annealing. The resistivity reduce 7.40% simultaneously result in inductance 14.3% decrease of spiral inductor (11). This result has much different from our experiment data which resistivity of Cu films decrease and inductance of spiral inductor is not change, simultaneously.

$$\frac{L_1 + \Delta L}{L_1} = \frac{L_2}{L_1} = \frac{{\rho_2}^2}{{\rho_1}^2} = \frac{(\rho_1 + \Delta\rho)^2}{{\rho_1}^2} \tag{11}$$

$$\Rightarrow 1 + \frac{\Delta L}{L_1} = 1 + 2\frac{\Delta\rho}{\rho_1} + \left(\frac{\Delta\rho}{\rho_1}\right)^2$$

$$\Rightarrow \frac{\Delta L}{L_1} = 2\frac{\Delta\rho}{\rho_1} + \left(\frac{\Delta\rho}{\rho_1}\right)^2$$

Substitution $\frac{\Delta\rho}{\rho_1} = -0.074$

$$\frac{\Delta L}{L_1} = 2(-0.074) + (-0.074)^2 = -0.143 = -14.3\%$$

Chapter 6 Summary and Future Works

6.1 Summary

The electrical resistivity of Cu films decrease about 7.40% after annealing at 600°C, but the inductance change has already thought the experimental error. The inductance did not change after annealing, therefore we conclusive that resistivity independent of inductance of on-chip spiral inductor. The independences matched with the prediction of Greenhouse thesis but totally contradicts with the model proposed by Chen et al.. And the relation between resistivity and inductance is not match with Chen's model of spiral inductor.

6.2 Future Works

The future work might place between the free electron density and the inductance of spiral inductor relations and he free electron density does not neglect on grain growth effect. It need to use Transmission electron microscopy (TEM) for knowing grain size change. And investigation the correlate between inductance, free electron density and grain size.

References

[1] Qing-Tang Jiang, Ming-Hsing Tsai and R. H. Havemann, Member, IEEE, “Line Width Dependence of Copper Resistivity”IEEE pp. 227-229, 2001.

[2] You-Lin Wu, Yi-Cheng Hwang, “Deuterium post-metallization anneal of electrochemical-plated Cu filmdeposited on different barrier materials” Science Direct, Thin Solid Films 461 pp.294-300, 2004

[3] Denny D. Tang, C. H. Diaz, C.P. Chao, Hunming Hsu, C.Y. Lee, C.S. Chang, Y.T. Chia, M.T.Yang, and JackY.C. Sun, Member, IEEE, “Foundry Technology for 130nm and beyond SoC” IEEE Custom Integrated Circuits Conference pp.15-5-1 - 15-5-8 2003.

[4] Qing-Tang Jiang, Ming-Hsing Tsai, Aaron Frank, Vijay Parihar, Matt Nowell, R. A. Augur, R. H. Havemann and J. D. Luttmer, “Annealing Impact on Damascene Cu Resistivity and Microstructures, ”IEEE pp.400-404, 2001.

[5] Qing-Tang Jiang, Aaron Frank, R. H. Havemann, Vijay Parihar and Matt Nowell, Member, IEEE “Optimization of Annealing conditions for Dual Damascene Cu Microstructures and Via Chain Yields” IEEE pp.139-140, 2001.

[6] K. Barmak, A. Gungor, C. Cabral, J. Harper, E. M. ,“Annealing behavior of Cu and dilute Cu-alloy films: Precipitation, grain growth, and resistivity” Journal of Applied Physics, Volume 94, Issue 3, pp. 1605-1616, 2003

[7] 1. E. Morifuji, A. Oishi, K. Miyashita, S. Aota, M. Nishigori, H. Ootani, T. Nakayama, K. Miyamoto, F. Matsuoka, T. Noguchi, and M. Kakumu, Member, IEEE “An 1.5 V High Performance Mixed Signal Integration with Indium Channel for 130nm Technology Node” IEEE pp.19.3.1-19.3.4, IEDM 2000.

[8] Richard M Forsythaustriamicrosystems “Mixed-signal Integrated Circuits for Low Power, Battery Driven Applications” October, 2004.

[9] C. C. Chen, J. K. Huang, and Y. T. Cheng, Member, IEEE, “A Closed-Form Integral Model of Apiral Inductor Using the Kramers-Kronig Relations”IEEE Microwave and Wireless components Letters, vol. 15, no. 11, pp. 778-780, Nov. 2005.

[10] John A. Rice, “*Mathematical Statistics and Data Analysis*”, California BROOKS/COLE

[11] Cutnell, John & Johnson, Kenneth. *Physics 4th edition*. New York: Wiley. 1998: 755.

[12] H. M. Greenhouse, “Design of Planar Rectangular Microelectronic Inductors”, IEEE trans Parts, Hybrids, Packag., vol. PHP-10, pp.101-109, June 1974.

Vita and Publication

姓名：賴文駿 (Wen-Chun Lai)

生日：中華民國七十年五月六日

電子郵件信箱：winjun.ee94g@nctu.edu.tw

學歷：

國立豐原高級中學 （1996.9.~1999.6）

（National Feng-yuan Senior High School）

國立清華大學數學系 （1999.6.~2005.6.）

（Department of Mathematics National Tsing-Hua University）

國立交通大學電子工程所碩士班 （2005.9.~2007.7.）

（Department of Electronics Engineering ＆ Institute of Electronics, National Chiao Tung University）